REVIEW

nature chemical biology

Imaging single events at the cell membrane

Jyoti K Jaiswal & Sanford M Simon

The ability to sense and respond to the environment is a hallmark of living systems. These processes occur at the levels of the organism, cells and individual molecules. Sensing of extracellular changes could result in a structural or chemical alteration in a molecule, which could in turn trigger a cascade of intracellular signals or regulated trafficking of molecules at the cell surface. These and other such processes allow cells to sense and respond to environmental changes. Often, these changes and the responses to them are spatially and/or temporally localized, and visualization of such events necessitates the use of high-resolution imaging approaches. Here we discuss optical imaging approaches and tools for imaging individual events at the cell surface with improved speed and resolution.

The use of ensemble measurements, which report changes that affect an averaged outcome, has been crucial in our understanding of transmembrane signaling. Such studies have identified various cell surface receptors and signaling mechanisms that detect and respond to extracellular signals, such as nutrients, growth factors, pathogens and the extracellular matrix. However, many physiological and pathological events affect individual molecules or organelles. Because information is lost by averaging signals, determining important mechanistic details necessitates studying individual events. For example, if a microscopic event exists in two or more states, such as a signaling cascade that is either on or off or an ion channel that is open or closed, the average will represent a state that does not exist at the microscopic level; averaging the amplitude of response thus results in a loss of information about individual events. As a second example, ensemble measurements report the dominant population but miss responses that occur from a minority of spatially or temporally localized signals. A third example is the inability to temporally order single events on the basis of an averaged measurement. Ordering the steps of a multistep process by ensemble study requires the individual events to be tightly synchronized, which is difficult to achieve and even more difficult to maintain. However, observing individual events allows the order of each step to be unambiguously determined without a need for synchronization. A fourth example is the loss of important temporal information about individual events in ensemble averages. Each molecule might alter its state exponentially over time, or the change might be abrupt but the distribution of when the change occurs among individual molecules might be exponential. The temporal nature of such microscopic events often cannot be resolved from ensemble measurements.

Many approaches have been developed to improve the spatial and temporal resolution with which we can study cellular and molecular responses at or near the cell surface. Approaches such as electron microscopy allow very high spatial resolution but are not suitable for imaging dynamic processes. Other approaches, such as scanning probe microscopy (which includes atomic force microscopy) and near-field scanning optical microscopy, offer spatial resolution at the nanometer scale. However, when scanning an area even as big as the surface of a cell, the temporal resolution becomes poor. Further, these methods do not allow simultaneous measurement of activities all across the cell surface, thus limiting their applicability for monitoring cell surface events in real time. The use of electrical measurements, such as voltage-clamp recording, allows membrane events to be studied at submillisecond temporal resolution. However, when performed at the whole-cell level, electrophysiology does not provide spatial information. Information on finer spatial detail can be gathered with patch-clamping to study single channels and transporters. However, this allows sampling at only a single spot. Since the introduction of patch-clamping three decades ago[1], it has been applied widely to study cell surface processes. Excellent discussion of these approaches, their applications and comparison with optical imaging are available[2–5] and will not be discussed here.

Many of the limits on spatial and temporal resolution can be overcome by optical imaging. Optical imaging permits monitoring from molecular to organismal scales and for time periods ranging from milliseconds to several days. In the first part of this review, we will discuss developments that have improved the speed and resolution of live cell imaging. In the second part, we will highlight the contributions and practical applications of these techniques to improve monitoring of single events at the cell membrane.

Tools for optimizing spatial and temporal resolution

Conventional optical microscopy allows an axial resolution of approximately 400 nm to be achieved. However, the cell membrane is two orders of magnitude smaller, at a thickness of approximately 4–6 nm (refs. 6–8) (**Fig. 1a**). This imposes two major impediments to monitoring single events in or near the cell membrane. First, the thinness of the membrane limits the number of fluorophores it can accommodate, and thus the intensity of the signal it can emit. Second, the membrane can contribute as little as 1% of the volume of each optical section, so even a small amount of noise from the cytoplasm can reduce the signal-to-noise ratio considerably.

Several approaches allow the reduction or elimination of out-of-plane fluorescence, and a few of these can surmount the physical limit imposed by the wavelength of visible light (**Fig. 1a**). This is achieved by

The Rockefeller University, 1230 York Avenue, New York, New York 10021, USA. Correspondence should be addressed to S.M.S. (simon@rockefeller.edu).

Published online 18 January 2007; doi:10.1038/nchembio855

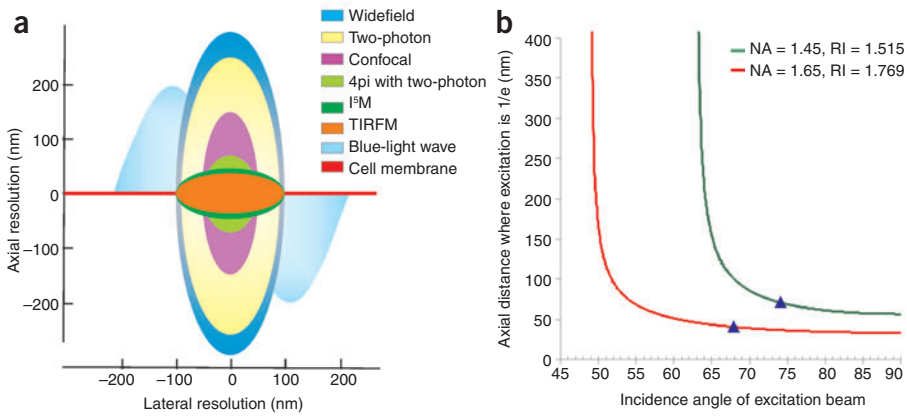

Figure 1 Resolution of various optical imaging approaches. (**a**) Estimated axial and lateral resolutions of various optical imaging approaches. The size of a single wave of blue light and axial thickness of cell membrane are drawn for the sake of comparison. The figure is partly redrawn with permission from ref. 61. (**b**) Distance over which the evanescent field decays to 1/e is a function of the refractive index of the glass and the angle of incidence of the excitation light. This has been drawn for two objectives, each with a different numerical aperture (NA) and refractive index (RI). The maximum angle that can be obtained by "through the objective" excitation is indicated by arrowheads for each objective.

using one or more of the following approaches: (i) discarding the light that originates from out-of-focus fluorophores (confocal microscopy), (ii) reassigning the in- and out-of-plane fluorescence to their respective locations by mathematical analyses (image deconvolution) and (iii) using illumination where the intensity varies nonlinearly with position (multiphoton microscopy, near-field scanning optical microscopy, evanescent wave microscopy and interference microscopy). Sometimes a combination of these approaches permits further enhancements in resolution, while other times physical properties of the fluorophores—such as resonant energy transfer or photoconversion—can be used to improve the limit of resolution[9,10]. In this section, we will discuss optical imaging approaches that use one or more of these features to improve spatial and temporal resolution.

Laser scanning microscopy. Confocal laser scanning microscopy is a common approach for reducing out-of-focus fluorescence, improving image contrast and, thus, improving detection ability. This imaging modality has been used extensively for improved three-dimensional imaging. Unlike wide-field microscopy, where both in- and out-of-focus light is collected, confocal microscopy uses a pinhole in the light path to discard out-of plane-light and improve image resolution. However, the scanning beam and repeated excitation of the sample in different optical planes result in extensive photobleaching and photodamage and slow image capture. These drawbacks for live cell imaging are minimized by the use of spinning-disk confocal microscopy. Here, instead of a single pinhole, a disk with multiple pinholes is used, generating a confocal image of the entire field of view. This image can be captured by a camera instead of by photomultiplier tube–based image reconstruction, thus speeding up the imaging. The use of a camera with high sensitivity allows the use of lower excitation intensity, thereby reducing photodamage. Together, these advances make spinning-disk microscopy better suited for imaging live cells. Deconvolution algorithms can be used to further improve the spatial resolution.

Light from out of the plane of focus can be independently reduced by decreasing the thickness of the excited region. One way to accomplish this is with two-photon laser illumination[11]. This approach requires the delivery of infrared photons in rapid pulses. Only those fluorophores that simultaneously absorb two of these photons are excited. The probability of this is proportional to the square of the intensity of excitation at any point. As the highest photon flux occurs at the laser focus, the excitation drops nonlinearly with distance from the focus. This effectively eliminates excitation (and thus unwanted light), as well as photobleaching and photodamage from out of the plane of focus. Because the wavelength of the infrared light is large, the use of infrared light for excitation in two-photon microscopy limits its axial resolution. However, by using a combination of two-photon and confocal imaging together with an appropriate dye, image resolution can be comparable to that of conventional confocal imaging. Moreover, reduced scattering of infrared light allows imaging of single events even deep within a tissue. Thus, two-photon imaging has been used for high-resolution, long-term imaging of individual vesicle exocytosis in live tissues[12].

Fluorescence correlation spectroscopy. Fluorescence correlation spectroscopy (FCS) is another approach for imaging single events[13]. In FCS, light is focused in a volume of approximately 10^{-15} l, and fluctuations in the fluorescence are recorded. These fluctuations are caused by random diffusion of fluorophores in and out of the illuminated region or by changes in their fluorescence emissions. This technique is used to determine the mass, density and rate of diffusion of an ensemble or an individual biomolecule, even at very low concentrations. FCS is particularly well suited for studying cell membrane events, as the cell membrane has lower spontaneous motion than do the cytoplasm and intracellular compartments (all of which can also be studied by FCS), and diffusion of molecules within the cell membrane is slower. FCS was first used three decades ago to study the behavior of molecules in the membrane bilayer[14] and has since been applied to study the behavior of single molecules in cell membranes[15].

The region imaged in FCS is orders of magnitude larger than the thickness of the cell membrane. When using FCS to study cell membrane events where the fluorophore does not localize exclusively to the cell membrane, a large amount of signal is collected from molecules not resident in the cell membrane. This could limit the utility of FCS. However, molecules in the cytoplasm diffuse in and out of the focal volume more rapidly than do molecules in the cell membrane, making it possible to reduce their contribution. The problem can be further reduced by decreasing the thickness of the illuminated region. One way to accomplish this is with two-photon laser illumination (described above) or by total internal reflection (TIR) excitation (described further in the next section), where excitation thickness can be an order of magnitude smaller than the wavelength of two-photon light. This provides superior resolution for cell surface imaging and, as such, TIR fluorescence microscopy (TIRFM) has itself been used widely for studying cell surface events[16–18].

TIRFM. TIRF or evanescent wave microscopy is based on the principle that when light traveling in a medium of high refractive index (such as glass) arrives at an interface with a medium of low refractive index (such as water or buffer), it totally is reflected back if it is above a critical angle. This causes a standing wave to form at the interface, in the medium with the lower refractive index. The intensity of this field decreases exponentially from the interface and is called an 'evanescent wave' (**Fig. 1b**). Thus,

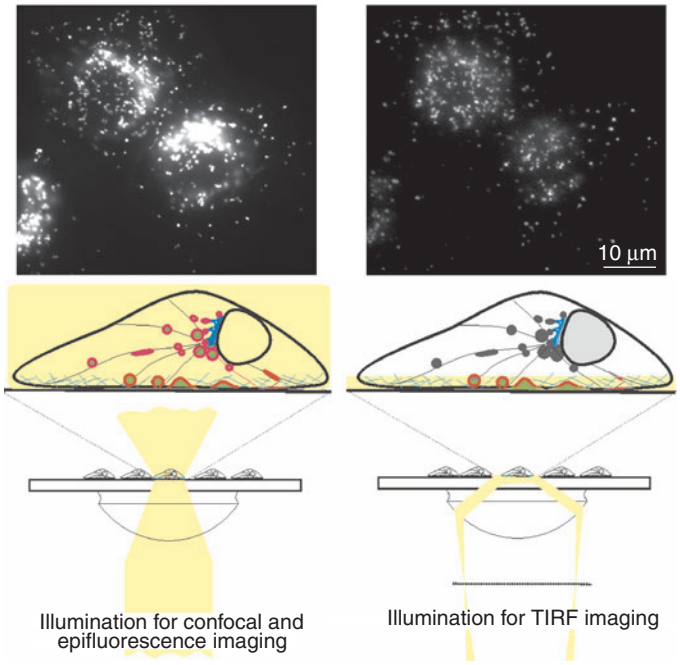

Figure 2 Comparison of wide-field and TIRF imaging. Lysosomes labeled with fluorescent dextran were imaged in the same focal plane by wide-field epifluorescence microscopy (top left) and TIRFM (top right). Images adapted with permission from *The Journal of Cell Biology*, 2002, **159**, 625-635. Copyright 2002 The Rockefeller University Press. In epifluorescence or confocal microscopy, laser light excites fluorophores throughout the cell (bottom left). In contrast, in TIRFM, the illumination decreases exponentially from the cover slip to 1/e within a distance roughly one quarter to one tenth of the wavelength of light (bottom right).

the closer the fluorophore is to the interface, the stronger the excitation. The distance over which fluorophores are efficiently excited by the evanescent wave can be altered by changing the incident angle of the light (**Fig. 1b**). This depth (the distance over which the intensity of excitation falls by 1/e) can range from 50 nm to 150 nm (**Fig. 1b**). This distance is less than the focal depth of a lens, which allows imaging of cell surface events with little or no out-of-focus fluorescence (**Fig. 2**). This not only improves the sensitivity of imaging but, by reducing the exposure of the bulk of the cell to excitation light, minimizes photodamage to the cell. Thus, TIRFM offers specific advantages for optical imaging of intra- and extracellular events at the cell surface.

TIR can be achieved using either a prism-based or objective-based setup. Each of these approaches has its own advantages, which have been discussed elsewhere[19,20]. Because it uses objectives with high numerical aperture, objective-based TIRFM is advantageous for detecting events where the number of photons is limiting[19,20]. The wide utility of this approach results largely from the suitability of TIRFM for high-resolution imaging and real-time imaging of cell surface events ranging in scale from single molecules to whole cells[16]. Recent technical advances and their incorporation in commercial TIRF microscopes are further expanding the utility of TIRFM[21].

Imaging below the diffraction limit. Several approaches allow imaging of fluorophores separated by distances smaller than the diffraction limit of visible light (**Fig. 1a**). These approaches include near-field scanning optical microscopy, stimulated emission depletion, 4pi, I^5M and saturated structured-illumination microscopy. The physical principles, advantages of these approaches and methods of setting them up have been described elsewhere. These approaches vary in the resolutions that they can achieve (**Fig. 1a**). It has been claimed that all of these approaches permit live cell imaging, although this has yet to be shown in the case of stimulated emission depletion microscopy. These are relatively new technologies, and their application for imaging cell surface events has only begun[22–24]. Approaches for nanometer-scale fluorescence imaging will substantially enhance the utility of fluorescence imaging for monitoring single events, so continued efforts are being made to develop them further.

Probes for fluorescent labeling

Improvements in fluorescent probes have also enhanced the utility of fluorescence imaging for studying cell surface events. Some of these advances include new variants of genetically encodable fluorescent proteins and new chemically synthesized probes[25,26]. These have been discussed in a number of recent reviews[27,28]. Additional probes include photoconvertible fluorescent proteins and quantum dots (QDs).

Photoconvertible fluorescent proteins. Once a fluorescent protein is synthesized, properly folded and made fluorescent through autocatalytic

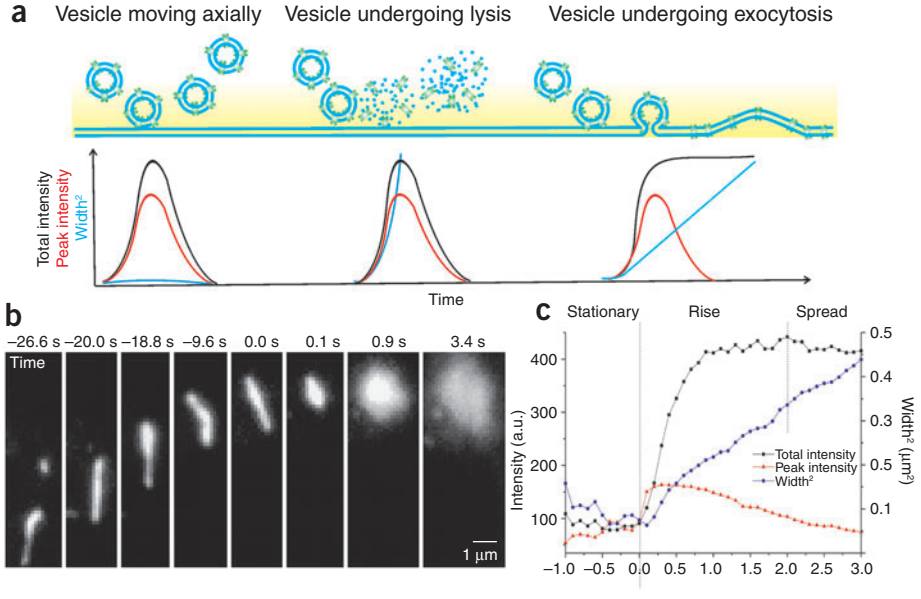

Figure 3 Use of TIRFM to study behavior of individual vesicles near the cell membrane. (**a**) Top panel shows three behaviors of vesicles near the cell surface as they enter the evanescent field (shaded yellow region). The vesicle in the left panel moves axially, entering the evanescent field and then retreating. The vesicle in the middle lyses upon entering the evanescent field. The vesicle on the right fuses to the membrane. Lower panel shows the predicted changes in peak intensity, total intensity and width of the fluorescence of the fluorescent cargo (green cylinders) in the membrane of the vesicle. (**b**) A single vesicle labeled with a GFP-tagged membrane protein (vesicular stomatitis virus glycoprotein) is observed to approach, move along the membrane, pause, and then undergo a lateral spread of its fluorescence[63]. (**c**) Quantification of fluorescence from the vesicle in **b**[63]. a.u., arbitrary units.

or chemical alterations, it remains so until photobleaching or degradation. This results in an excess of labeled proteins, which makes it difficult to identify and follow single events. The use of fluorescence recovery after photobleaching, a technique that relies on localized photobleaching, has added a temporal dimension that facilitates the monitoring of cell surface protein trafficking[29]. Recently, proteins whose fluorescence can be regulated, increased in intensity (photoactivation) or changed in color (photoconversion) by light of specific wavelengths have been developed[30]. This permits light-mediated localized tagging of molecules in a diffraction-limited region inside or at the surface of the cell. Once labeled, many of the photoproteins remain converted and can be followed[31,32].

Another application of these probes is in increasing the imaging resolution. Using the photoconvertible protein FP595, nanometer imaging resolution of 50–100 nm has been achieved[33,34]. Another recent approach, stochastic optical reconstruction microscopy, uses TIRF imaging together with photoswitching of fluorophores to image at 20-nm resolution[10]. Besides these, the ability to photoregulate opens up other possibilities for improving the resolution of imaging of even the wide-field microscope: when combined with fluorescence resonance energy transfer imaging and localized photoactivation at the cell surface, it allows the use of wide-field imaging to selectively monitor interactions of specific cell surface proteins with appropriately tagged cytosolic proteins.

QDs. QDs are nanometer-scale crystals made of semiconductor materials. These inorganic fluorophores are bright and highly resistant to photobleaching, have broad excitation spectra and can be synthesized with narrow emission spectra centered almost anywhere in the visual spectrum. These features make it easy to identify and track single QDs and simultaneously track multiple QDs, each with a different color emission. QDs are thus well suited for fluorescence imaging of single events. QDs do not pass through the cell membrane and can be readily used to label lipids, proteins and other cell surface molecules by conjugation to a specific ligand or antibody to target the molecule of interest[35,36]. Labeling of intracellular targets requires delivery of the QDs into cells. Techniques that have been used for this purpose include cationic lipids, cell-penetrating peptides and microinjection[35].

Metals such as cadmium and selenium are used in the synthesis of QDs. Concerns have therefore been raised about potential adverse effects of QDs on live cells. However, several studies have pointed out that this may not be detrimental as long as the QD cores are capped appropriately[36,37]. Also, several organic polymers that make QDs stable in a hydrophilic environment have not been found to have detectable effects on cellular physiology[38]. Other concerns regarding the use of QDs remain. These include the size of hydrophilic QDs, which ranges from 10 nm to 20 nm for some of the commercially available QDs. This makes them considerably larger than most fluorescent organic dyes and larger than some of the fluorescent proteins. Further limitations are the tendency of QDs to aggregate and the inability of current approaches to permit monovalent labeling of biomolecules with QDs. Here again, some progress has been made, such as the use of polyethylene glycol to coat the QD surface and

BOX 1 MONITORING THE FATE OF INDIVIDUAL VESICLES AT THE CELL MEMBRANE BY TIRFM

TIRF imaging permits the monitoring of various steps and fates of vesicles at the cell membrane. This requires monitoring of the movement of the fluorescent vesicle, its total emission intensity, its peak emission intensity and the width of its intensity profile. Submicron-scale lateral movement of the fluorescent vesicle can be readily detected during real-time imaging by changes in its *x* and *y* coordinates[64,65]. As the TIRF excitation intensity decays exponentially along the *z* axis, axial movement of the vesicle toward the cell membrane results in a rapid increase in its total fluorescence intensity. This has been used to monitor movements on the scale of tens of nanometers[65].

The ability to monitor movement at this spatial resolution allows the identification of docked vesicles. Thus, monitoring of total or maximal fluorescence by TIRF imaging allows the monitoring of vesicle trafficking and docking. Distinguishing a vesicle that fuses from one that lyses is less straightforward. In both cases, the vesicle appears to become brighter as it approaches the membrane, then rapidly dimmer as a result of release of its luminal contents by either lysis or exocytosis (**Fig. 3a**). This can be resolved by labeling the vesicle membrane and monitoring two critical features:

- Relative change in peak and total fluorescence. As a fusing vesicle starts to flatten out, the fluorophores on its distal surface are better excited, causing an increase in both total and peak fluorescence. This will be followed by a period in which total fluorescence remains constant (as they are now in the plasma membrane; **Fig. 3b** and black line in **Fig. 3a**,**c**), whereas the peak fluorescence decreases (because the fluorophores are spreading laterally in the cell membrane; **Fig. 3b** and red line in **Fig. 3a**,**c**). However, if the vesicle lyses, the fluorophores are released in the cytoplasm, causing the peak and total fluorescence to decrease simultaneously.
- Lateral spread of fluorescence. Only if the fluorophores from the vesicle are delivered to the membrane will the fluorescence spread radially, as would be expected by diffusion into a two-dimensional membrane (blue line in **Fig. 3a**,**c**). As a result, the area occupied by the fluorophores would increase linearly with time. The slope of this line should be the known two-dimensional diffusion constant of that marker.

For similar reasons, TIRFM is also suitable for monitoring individual endocytic vesicles as they bud and retrieve molecules at the cell surface. Endocytosis of fluorescently tagged cargo (cell surface proteins or lipids or extracellular ligands) results in gradual disappearance of its fluorescence from the TIR field as the vesicle carrying it moves deeper into the cell. However, photobleaching or movement of the cell membrane (not of the vesicle) could also result in a gradual decrease in fluorescence, making it important to distinguish these processes. Axial motion of the cell membrane could be detected by simultaneously monitoring a cell membrane–specific marker together with the marker for the endocytic vesicle[66]. Endocytosis and photobleaching can be distinguished in two ways. One is to monitor the endocytic vesicle alternately with TIRFM and wide-field microscopy[67]. An endocytic vesicle will disappear from the TIRF field as it moves over 100 nm axially from the cell membrane (**Fig. 1b**). However, as this is below the axial resolution limit of the wide-field microscope, this vesicle could still be observed by wide-field microscopy until it moves out of the focal plane (**Fig. 1a**). In contrast, disappearance of a vesicle because of photobleaching or disassembly of components will result in its simultaneous absence from both TIRF and wide-field images. Another approach to identifying an endocytic vesicle involves monitoring whether multiple components of endocytic machinery (such as clathrin or adaptors) and/or cargo disappear simultaneously and at the same rate at the same spot on the membrane[68,69].

minimize the tendency of QDs to aggregate, and the conjugation of molecules with QDs at substoichiometric concentrations of the ligand to minimize multivalent conjugations[39]. Further advances are still needed to improve the utility of QDs in imaging single events at the cell surface. These include the synthesis of monovalent QDs for labeling of single molecules, a reduction in the size of biofunctional QDs, and the development of approaches for covalent labeling of molecules with QDs in live cells.

Applying these tools to image cell surface events

Imaging of single events offers novel insights regarding how a cell finely regulates its communication with the environment and surrounding cells. As an example, cell surface molecule trafficking is regulated by delivery (exocytic) and retrieval (endocytic) systems, which in turn affect each other. Imaging of exocytosis of single vesicles allows us to evaluate various aspects of membrane protein trafficking models. The observation that membrane fusion and mixing may not go to completion after the initiation of membrane mixing challenges the belief that exocytosis is regulated only until merger of the two opposing membranes has been initiated. It has been proposed that this process, called partial or 'kiss and run' fusion, is used by cells to regulate the amount of release or allow size-selective delivery of cargo[40–42]. Monitoring of single-vesicle trafficking events has shown that selective retention of cargo also has a role in segregation of endocytosed cargo during maturation of endosomes and recycling of endocytosed cargo[43,44]. In the following section, we will describe how the above-mentioned approaches have been applied to monitoring individual events at the cell surface.

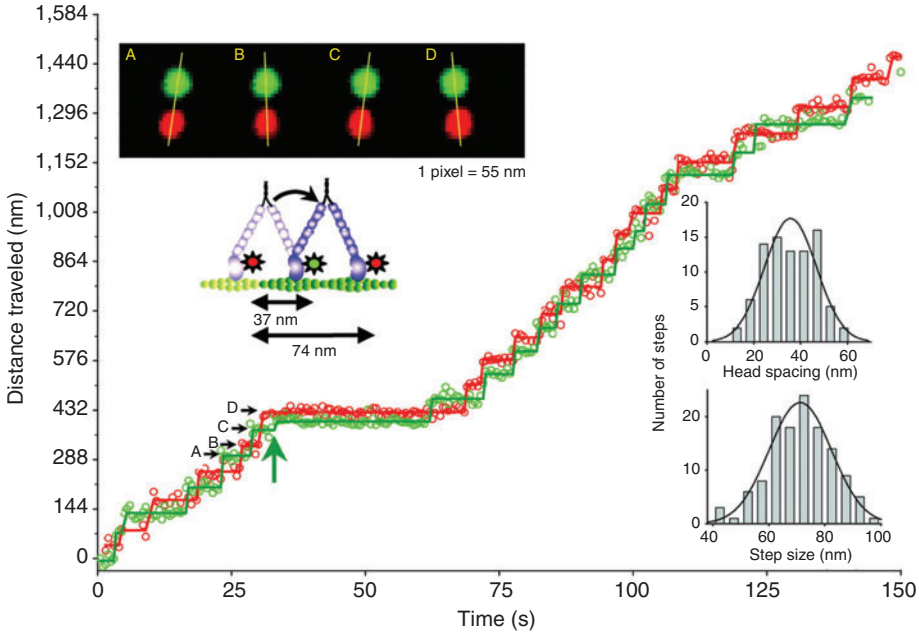

Figure 4 Myosin V processive run with heads labeled with QDs of different colors. Green and red open circles in main graph indicate QD (565 nm) and QD (655 nm) positions, respectively, determined by Gaussian fits. Solid lines indicate average QD positions between steps, with the onset of steps determined by eye. Top left inset shows averaged QD images for steps labeled A–D in graph, with red and green images offset by 12 pixels in *y* axis for clarity. The yellow lines connect QD centers, emphasizing alternating relative head positions. Green arrow in main graph identifies substep. Lower right inset shows histograms of interhead spacing and step size. Reproduced with permission from ref. 54.

Monitoring the trafficking of cell surface molecules. Vesicles deliver molecules at the cell surface by exocytosis and retrieve molecules from the cell surface by endocytosis. The final steps of the life of an exocytic vesicle can be classified into the following stages: transport to the cell membrane, engagement at the membrane with molecules necessary for fusion (docking), and delivery of its contents at the cell membrane (fusion). Each of those stages can be monitored for a single vesicle using a combination of quantitative image analysis and high-resolution light microscopy approaches. Of these approaches, TIRFM is most widely applied for this purpose[45,46] because of its ability to selectively monitor vesicles near the cell membrane (**Fig. 3a**). The high signal-to-noise ratio permits rapid imaging with lower light intensity, minimizing photodamage. In addition, as described in **Box 1**, use of TIRF imaging allows us to distinguish vesicles that undergo fusion (**Fig. 3b**,**c**) from those that are damaged by light or other means, resulting in their lysis (**Fig. 3a**).

A limitation of TIRF imaging is that it can monitor exocytic and endocytic events only at the basal surface of the cell. Laser scanning and spinning-disk confocal microscopy have been used to monitor vesicles inside and at other surfaces in the cell[47–50]. However, the signal-to-noise ratio that can be achieved with these microscopy approaches is lower, and their axial resolution is limited by diffraction. Poor signal-to-noise ratios result in missing events where the emission intensity is relatively weak, and lower resolution makes it difficult to unambiguously distinguish a vesicle at the cell surface from one adjacent to it. Together, these limitations cause ambiguities in studies of the fate of individual endo- and exocytic vesicles. For this reason, wherever applicable, TIRFM is the method of choice to monitor the fate of individual vesicles at the cell surface.

Probes such as photoactivated green fluorescent protein (PA-GFP) that are photoregulated in only a small portion of the cell can further aid in monitoring individual trafficking events at the cell surface. In one study, PA-GFP was used to examine the localization and diffusion behavior of two different types of potassium channels[51]. In another study, the human immunodeficiency virus protein Nef was tagged with PA-GFP to track its fate after endocytosis[52]. These studies were carried out using confocal microscopy, and probes in a large area of the cell were activated. To selectively activate the fluorescence in the cell membrane, photoactivation could be carried out using TIRFM or interference microscopy, which would add to the utility of these probes for monitoring cell surface events. Besides photoconvertible probes, QDs are also useful for monitoring single membrane trafficking events at high resolution. In one such example, QDs were used to study the endocytosis of epidermal growth factor (EGF) receptor[53].

Tracking single molecules on the cell surface. Properties of cell surface molecules are regulated by changes in their distribution or interactions with other molecules. Monitoring the behavior of individual molecules at the cell surface is thus important for understanding their function(s). Probes used for this purpose must have high specificity and monovalency (one probe should only bind one molecule, and vice versa) and the ability to resist photodamage and metabolic degradation. This can be achieved by genetically labeling the target protein by expressing it as a fusion with a fluorescent protein or a peptide that can

BOX 2 PHOTOPHYSICAL PROPERTIES OF FLUOROPHORES THAT ALLOW IDENTIFICATION OF A SINGLE FLUOROPHORE

- Fluorescence intensity. The observed emission intensity of the fluorophores should be consistent with that of a single fluorophore, with variations in intensity being multiples of this minimal value (quanta).
- Fluorescence blinking. If the environment is kept constant, the fluorescence should have only two emission levels (on or off). In the case of photoconvertible fluorophores such as DRONPA, besides blinking, even the intensity of emission upon photoconversion should be quantized[70].
- Single-step photobleaching. When the fluorophore turns off irreversibly because of photobleaching, this event should occur without intermediate levels of emission.
- Emission dipole. If the fluorescent probe is immobilized, its absorption and emission dipole should be defined[71].
- Antibunching effect. When single-photon emission can be monitored, it should be determined that simultaneous emission of two photons does not occur[72].

bind fluorophores[26]. When labeling a molecule chemically, approaches are needed to ensure one-to-one pairing of the probe and the molecule of interest. This is crucial for the purpose of monitoring individual cell surface events, as multivalent labeling itself can affect the distribution and properties of the molecule of interest, which could in turn alter the cell's signaling and physiology.

Regardless of labeling strategy, there is a need to establish that the signal being monitored is from a single fluorescent probe. This can be done by monitoring various photophysical properties of fluorescent probes, which are described in **Box 2**. In a cellular context, extraneous factors often confound reliable measurement of these parameters, making it necessary to test as many of these features as possible. A requirement that is central to all single-molecule measurements is a high signal-to-noise ratio. Because of their brightness and high photostability, QDs provide a high signal-to-noise ratio and have been used for imaging of single molecules. In one such study, QDs of two different colors were used to label each of the two arms of a myosin V molecule, and the movement of individual molecules along the actin bundle was followed *in vitro* (**Fig. 4**)[54]. Similar attempts have been made to monitor individual molecules in live cells[55,56]. However, these studies did not test the parameters described in **Box 2** to establish that single QDs were being imaged. Further, a one-to-one binding of QD to protein was not shown. While success in monitoring single QDs *in vitro* leaves little doubt that this should be achievable in cellular contexts as well, such studies should be examined rigorously.

Besides the probe, the choice of imaging approach also affects the signal-to-noise ratio and thus the ability to measure the parameters required for identifying single molecules. Approaches such as TIRF, 4pi and I^5M microscopy, which reduce background by permitting excitation of regions below the diffraction limit, significantly improve the ratio of signal to noise. These approaches can be used to image and track individual molecules on the cell surface. However, if tracking of the molecule is not required, these approaches can be combined with FCS to monitor the properties of individual molecules and their interactions with other molecules. In one such study, FCS was used to monitor the interaction of EGF with its receptor in live cells[57]. Similarly, a combination of TIRFM and FCS has been used to study interactions of a variety of ligand-receptor pairs in model membrane systems[58]. In another study, conventional FCS was used to monitor diffusion of lipids in cell and artificial membranes to study the presence of lipid microdomains (rafts) in the presence of cholesterol[59]. Finally, a combination of TIRFM and FCS allowed the study of binding between cell membrane and membrane lipid-binding proteins in live cells[60].

Conclusion

The new tools and techniques discussed here, many of which are still in development, hold the potential to significantly alter the resolution and precision with which single events can be monitored at the cell membrane. Such studies have already started offering new insights into the mechanisms and roles of these events in regulating the physiology of a cell and its ability to communicate with other cells. Further technological developments in this vein are bound to increase our understanding of the interactions between the cell's interior and exterior by allowing us to study the events that occur at the cell membrane.

ACKNOWLEDGMENTS

Work in our laboratory is supported by grants from the National Science Foundation (NSF FEB 00520813) and the National Institutes of Health (P20 GM072015 and GM072015 to S.M.S.). We thank P. Coffino for helpful comments on the manuscript.

COMPETING INTERESTS STATEMENT

The authors declare that they have no competing financial interests.

Published online at http://www.nature.com/naturechemicalbiology
Reprints and permissions information is available online at http://npg.nature.com/reprintsandpermissions

1. Neher, E. & Sakmann, B. Single-channel currents recorded from membrane of denervated frog muscle fibres. *Nature* **260**, 799–802 (1976).
2. Sakmann, B. & Neher, E. Patch clamp techniques for studying ionic channels in excitable membranes. *Annu. Rev. Physiol.* **46**, 455–472 (1984).
3. Sakmann, B. Elementary steps in synaptic transmission revealed by currents through single ion channels. *Science* **256**, 503–512 (1992).
4. Angleson, J.K. & Betz, W.J. Monitoring secretion in real time: capacitance, amperometry and fluorescence compared. *Trends Neurosci.* **20**, 281–287 (1997).
5. Mosharov, E.V. & Sulzer, D. Analysis of exocytotic events recorded by amperometry. *Nat. Methods* **2**, 651–658 (2005).
6. Ruta, V., Chen, J. & MacKinnon, R. Calibrated measurement of gating-charge arginine displacement in the KvAP voltage-dependent K+ channel. *Cell* **123**, 463–475 (2005).
7. White, S.H., Ladokhin, A.S., Jayasinghe, S. & Hristova, K. How membranes shape protein structure. *J. Biol. Chem.* **276**, 32395–32398 (2001).
8. Gandhavadi, M., Allende, D., Vidal, A., Simon, S.A. & McIntosh, T.J. Structure, composition, and peptide binding properties of detergent soluble bilayers and detergent resistant rafts. *Biophys. J.* **82**, 1469–1482 (2002).
9. Sekar, R.B. & Periasamy, A. Fluorescence resonance energy transfer (FRET) microscopy imaging of live cell protein localizations. *J. Cell Biol.* **160**, 629–633 (2003).
10. Rust, M., Bates, M. & Zhuang, X. Sub-diffraction-limit imaging by stochastic optical reconstruction microscopy (STORM). *Nat. Methods* **3**, 793–795 (2006).
11. Denk, W., Strickler, J.H. & Webb, W.W. Two-photon laser scanning fluorescence microscopy. *Science* **248**, 73–76 (1990).
12. Takahashi, N., Kishimoto, T., Nemoto, T., Kadowaki, T. & Kasai, H. Fusion pore dynamics and insulin granule exocytosis in the pancreatic islet. *Science* **297**, 1349–1352 (2002).
13. Webb, W.W. Applications of fluorescence correlation spectroscopy. *Q. Rev. Biophys.* **9**, 49–68 (1976).
14. Fahey, P.F. *et al.* Lateral diffusion in planar lipid bilayers. *Science* **195**, 305–306 (1977).
15. Schwille, P., Korlach, J. & Webb, W.W. Fluorescence correlation spectroscopy with single-molecule sensitivity on cell and model membranes. *Cytometry* **36**, 176–182 (1999).
16. Axelrod, D. Total internal reflection fluorescence microscopy in cell biology. *Traffic* **2**, 764–774 (2001).
17. Axelrod, D. Cell-substrate contacts illuminated by total internal reflection fluorescence. *J. Cell Biol.* **89**, 141–145 (1981).
18. Axelrod, D., Burghardt, T.P. & Thompson, N.L. Total internal reflection fluorescence.

Annu. Rev. Biophys. Bioeng. **13**, 247–268 (1984).
19. Kawano, Y. *et al.* High-numerical-aperture objective lenses and optical system improved objective type total internal reflection fluorescence microscopy. *Proc. SPIE* **4098**, 142–151 (2000).
20. Axelrod, D. Selective imaging of surface fluorescence with very high aperture microscope objectives. *J. Biomed. Opt.* **6**, 6–13 (2001).
21. Schneckenburger, H. Total internal reflection fluorescence microscopy: technical innovations and novel applications. *Curr. Opin. Biotechnol.* **16**, 13–18 (2005).
22. Kittel, R.J. *et al.* Bruchpilot promotes active zone assembly, Ca2+ channel clustering, and vesicle release. *Science* **312**, 1051–1054 (2006).
23. Willig, K.I., Rizzoli, S.O., Westphal, V., Jahn, R. & Hell, S.W. STED microscopy reveals that synaptotagmin remains clustered after synaptic vesicle exocytosis. *Nature* **440**, 935–939 (2006).
24. Sieber, J.J., Willig, K.I., Heintzmann, R., Hell, S.W. & Lang, T. The SNARE motif is essential for the formation of syntaxin clusters in the plasma membrane. *Biophys. J.* **90**, 2843–2851 (2006).
25. Shaner, N.C., Steinbach, P.A. & Tsien, R.Y. A guide to choosing fluorescent proteins. *Nat. Methods* **2**, 905–909 (2005).
26. Giepmans, B.N., Adams, S.R., Ellisman, M.H. & Tsien, R.Y. The fluorescent toolbox for assessing protein location and function. *Science* **312**, 217–224 (2006).
27. Tsien, R.Y. The green fluorescent protein. *Annu. Rev. Biochem.* **67**, 509–544 (1998).
28. Griesbeck, O. Fluorescent proteins as sensors for cellular functions. *Curr. Opin. Neurobiol.* **14**, 636–641 (2004).
29. Lippincott-Schwartz, J. & Smith, C.L. Insights into secretory and endocytic membrane traffic using green fluorescent protein chimeras. *Curr. Opin. Neurobiol.* **7**, 631–639 (1997).
30. Lukyanov, K.A., Chudakov, D.M., Lukyanov, S. & Verkhusha, V.V. Innovation: photoactivatable fluorescent proteins. *Nat. Rev. Mol. Cell Biol.* **6**, 885–891 (2005).
31. Lippincott-Schwartz, J., Altan-Bonnet, N. & Patterson, G.H. Photobleaching and photoactivation: following protein dynamics in living cells. *Nat. Cell Biol.* Suppl, S7–S14 (2003).
32. Chudakov, D.M. & Lukyanov, K.A. Use of green fluorescent protein (GFP) and its homologs for *in vivo* protein motility studies. *Biochemistry (Mosc.)* **68**, 952–957 (2003).
33. Hofmann, M., Eggeling, C., Jakobs, S. & Hell, S.W. Breaking the diffraction barrier in fluorescence microscopy at low light intensities by using reversibly photoswitchable proteins. *Proc. Natl. Acad. Sci. USA* **102**, 17565–17569 (2005).
34. Betzig, *et al.* Imaging intracellular fluorescent proteins at nanometer resolution. *Science* **313**, 1642–1645 (2006).
35. Jaiswal, J.K., Goldman, E.R., Mattoussi, H. & Simon, S.M. Use of quantum dots for live cell imaging. *Nat. Methods* **1**, 73–78 (2004).
36. Jaiswal, J.K. & Simon, S.M. Potentials and pitfalls of fluorescent quantum dots for biological imaging. *Trends Cell Biol.* **14**, 497–504 (2004).
37. Gao, X. *et al. In vivo* molecular and cellular imaging with quantum dots. *Curr. Opin. Biotechnol.* **16**, 63–72 (2005).
38. Michalet, X. *et al.* Quantum dots for live cells, *in vivo* imaging, and diagnostics. *Science* **307**, 538–544 (2005).
39. Uyeda, H.T., Medintz, I.L., Jaiswal, J.K., Simon, S.M. & Mattoussi, H. Synthesis of compact multidentate ligands to prepare stable hydrophilic quantum dot fluorophores. *J. Am. Chem. Soc.* **127**, 3870–3878 (2005).
40. An, S. & Zenisek, D. Regulation of exocytosis in neurons and neuroendocrine cells. *Curr. Opin. Neurobiol.* **14**, 522–530 (2004).
41. Palfrey, H.C. & Artalejo, C.R. Secretion: kiss and run caught on film. *Curr. Biol.* **13**, R397–R399 (2003).
42. Jaiswal, J.K., Chakrabarti, S., Andrews, N.W. & Simon, S.M. Synaptotagmin VII restricts fusion pore expansion during lysosomal exocytosis. *PLoS Biol.* **2**, E233 (2004).
43. Rink, J., Ghigo, E., Kalaidzidis, Y. & Zerial, M. Rab conversion as a mechanism of progression from early to late endosomes. *Cell* **122**, 735–749 (2005).
44. Lampson, M.A., Schmoranzer, J., Zeigerer, A., Simon, S.M. & McGraw, T.E. Insulin-regulated release from the endosomal recycling compartment is regulated by budding of specialized vesicles. *Mol. Biol. Cell* **12**, 3489–3501 (2001).
45. Oheim, M., Loerke, D., Stuhmer, W. & Chow, R.H. The last few milliseconds in the life of a secretory granule. Docking, dynamics and fusion visualized by total internal reflection fluorescence microscopy (TIRFM). *Eur. Biophys. J.* **27**, 83–98 (1998).
46. Steyer, J.A., Horstmann, H. & Almers, W. Transport, docking and exocytosis of single secretory granules in live chromaffin cells. *Nature* **388**, 474–478 (1997).
47. Kreitzer, G. *et al.* Three-dimensional analysis of post-Golgi carrier exocytosis in epithelial cells. *Nat. Cell Biol.* **5**, 126–136 (2003).
48. Ma, L. *et al.* Direct imaging shows that insulin granule exocytosis occurs by complete vesicle fusion. *Proc. Natl. Acad. Sci. USA* **101**, 9266–9271 (2004).
49. Ehrlich, M. *et al.* Endocytosis by random initiation and stabilization of clathrin-coated pits. *Cell* **118**, 591–605 (2004).
50. Ohara-Imaizumi, M. *et al.* Monitoring of exocytosis and endocytosis of insulin secretory granules in the pancreatic beta-cell line MIN6 using pH-sensitive green fluorescent protein (pHluorin) and confocal laser microscopy. *Biochem. J.* **363**, 73–80 (2002).
51. O'Connell, K.M. & Tamkun, M.M. Targeting of voltage-gated potassium channel isoforms to distinct cell surface microdomains. *J. Cell Sci.* **118**, 2155–2166 (2005).
52. Massol, R.H., Larsen, J.E. & Kirchhausen, T. Possible role of deep tubular invaginations of the plasma membrane in MHC-I trafficking. *Exp. Cell Res.* **306**, 142–149 (2005).
53. Lidke, D.S., Lidke, K.A., Rieger, B., Jovin, T.M. & Arndt-Jovin, D.J. Reaching out for signals: filopodia sense EGF and respond by directed retrograde transport of activated receptors. *J. Cell Biol.* **170**, 619–626 (2005).
54. Warshaw, D.M. *et al.* Differential labeling of myosin V heads with quantum dots allows direct visualization of hand-over-hand processivity. *Biophys. J.* **88**, L30–L32 (2005).
55. Dahan, M. *et al.* Diffusion dynamics of glycine receptors revealed by single-quantum dot tracking. *Science* **302**, 442–445 (2003).
56. Courty, S., Luccardini, C., Bellaiche, Y., Cappello, G. & Dahan, M. Tracking individual kinesin motors in living cells using single quantum-dot imaging. *Nano Lett.* **6**, 1491–1495 (2006).
57. Pramanik, A. & Rigler, R. Ligand-receptor interactions in the membrane of cultured cells monitored by fluorescence correlation spectroscopy. *Biol. Chem.* **382**, 371–378 (2001).
58. Lieto, A.M., Cush, R.C. & Thompson, N.L. Ligand-receptor kinetics measured by total internal reflection with fluorescence correlation spectroscopy. *Biophys. J.* **85**, 3294–3302 (2003).
59. Bacia, K., Scherfeld, D., Kahya, N. & Schwille, P. Fluorescence correlation spectroscopy relates rafts in model and native membranes. *Biophys. J.* **87**, 1034–1043 (2004).
60. Ohsugi, Y., Saito, K., Tamura, M. & Kinjo, M. Lateral mobility of membrane-binding proteins in living cells measured by total internal reflection fluorescence correlation spectroscopy. *Biophys. J.* **91**, 3456–3464 (2006).
61. Gustafsson, M.G. Extended resolution fluorescence microscopy. *Curr. Opin. Struct. Biol.* **9**, 627–634 (1999).
62. Jaiswal, J.K., Andrews, N.W. & Simon, S.M. Membrane proximal lysosomes are the major vesicles responsible for calcium-dependent exocytosis in nonsecretory cells. *J. Cell Biol.* **159**, 625–635 (2002).
63. Schmoranzer, J., Goulian, M., Axelrod, D. & Simon, S.M. Imaging constitutive exocytosis with total internal reflection fluorescence microscopy. *J. Cell Biol.* **149**, 23–32 (2000).
64. Johns, L.M., Levitan, E.S., Shelden, E.A., Holz, R.W. & Axelrod, D. Restriction of secretory granule motion near the plasma membrane of chromaffin cells. *J. Cell Biol.* **153**, 177–190 (2001).
65. Allersma, M.W., Bittner, M.A., Axelrod, D. & Holz, R.W. Motion matters: secretory granule motion adjacent to the plasma membrane and exocytosis. *Mol. Biol. Cell* **17**, 2424–2438 (2006).
66. Rappoport, J.Z., Taha, B.W. & Simon, S.M. Movement of plasma-membrane-associated clathrin spots along the microtubule cytoskeleton. *Traffic* **4**, 460–467 (2003).
67. Merrifield, C.J., Feldman, M.E., Wan, L. & Almers, W. Imaging actin and dynamin recruitment during invagination of single clathrin-coated pits. *Nat. Cell Biol.* **4**, 691–698 (2002).
68. Merrifield, C.J., Perrais, D. & Zenisek, D. Coupling between clathrin-coated-pit invagination, cortactin recruitment, and membrane scission observed in live cells. *Cell* **121**, 593–606 (2005).
69. Rappoport, J.Z., Benmerah, A. & Simon, S.M. Analysis of the AP-2 adaptor complex and cargo during clathrin-mediated endocytosis. *Traffic* **6**, 539–547 (2005).
70. Habuchi, S. *et al.* Reversible single-molecule photoswitching in the GFP-like fluorescent protein Dronpa. *Proc. Natl. Acad. Sci. USA* **102**, 9511–9516 (2005).
71. Sosa, H., Peterman, E.J., Moerner, W.E. & Goldstein, L.S. ADP-induced rocking of the kinesin motor domain revealed by single-molecule fluorescence polarization microscopy. *Nat. Struct. Biol.* **8**, 540–544 (2001).
72. Basche, T., Moerner, W.E., Orrit, M. & Talon, H. Photon antibunching in the fluorescence of a single dye molecule trapped in a solid. *Phys. Rev. Lett.* **69**, 1516–1519 (1992).